Scalable microfluidic platform for flexible configuration of, and experiments with microtissue multi-organ models.

Supplementary Material

Christian Lohasz[1], Nassim Rousset[1], Kasper Renggli[1], Andreas Hierlemann[1] and Olivier Frey[1, 2]

[1]Eidgenössische Technische Hochschule Zürich, Department of Biosystems Science and Engineering, Bio Engineering Laboratory, Basel, Switzerland

[2]InSphero AG, Schlieren Switzerland

Supplementary Methods

Computational Modeling

The numerical model combines a matrix implementation of hydraulic-electric analogy with Kirchhoff's law to find flow rates and pressures in each channel and at each point in the device. Subsequently, a time-stepping scheme is implemented with the forward Euler method to establish the flow transients through all components of the chip.

The hydraulic-electric analogy models (i) each channel as a hydraulic resistance, (ii) each drop with a given curvature as a pressure source due to their Laplace pressure, and (iii) all components with a height greater than that of the channel – from the inlet-outlet to each individual MT compartment – as pressure sources due to gravity. (i) Hydraulic resistances are found by importing the device structure in COMSOL Multiphysics® and using the Laminar Flow module. (ii) The volume in the drop dictates its radius,R, which, with surface tension γ, generates a Laplace pressure $\Delta P_{Lap} = \gamma/2R$. (iii) Due to gravity g and the liquid density,ρ, the height h above the channel generates a pressure $\Delta P_g = \rho gh$.

The equivalent circuit is composed of pressure sources at open drops and reservoirs, nodes at each MT compartment, and hydraulic resistances between all nodes and pressure sources. Each pressure source has a known pressure given by the volume contained in it: Standing drops have a pressure given by their capillary radius, dependent on the volume, and by the height of the MT compartment; the inlet and outlet exert a certain pressure on the system depending on the tilting angle and on how much volume they contain. Writing the equations in a matrix form (Kirchhoff's law) enables to find the unknown inter-nodal flow rates and nodal pressures for a given volume contained in drops and reservoirs.

The time-stepping scheme uses the previously established flow rates to update the volume in drops and reservoirs iteratively over time. In turn, this affects the pressure in the system, i.e., the resulting flow rate. Ultimately, the flow transients for a given tilting angle are found, with which we derive the maximum flow rate and the time during which a specific angle can be held (Figure 4 simulation results).

Supplementary Figures

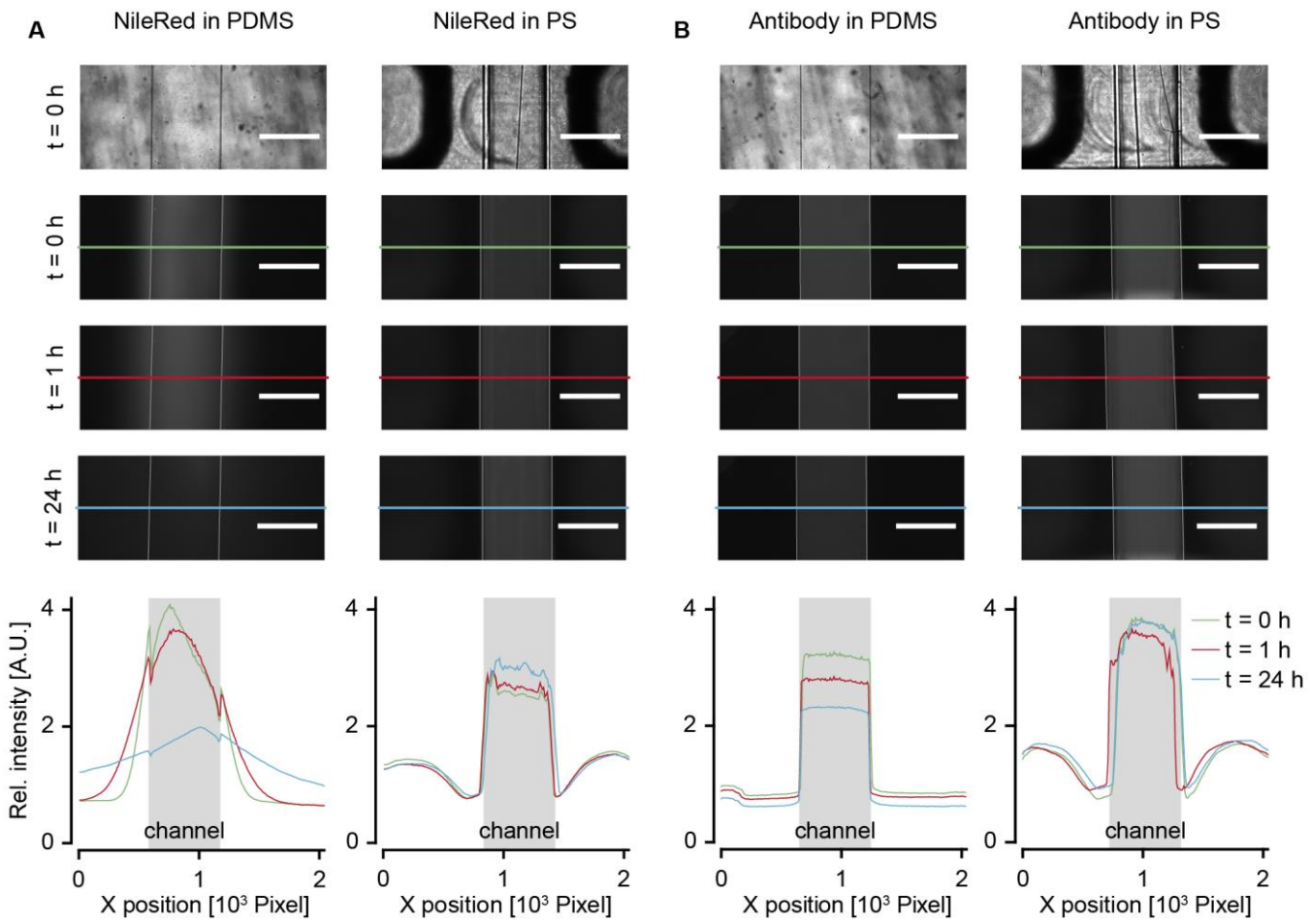

Supplementary Figure 1: Absorption of substances in polydimethylsiloxane (PDMS) and polystyrene (PS). (A) NileRed and (B) Cy3-conjugated antibodies were loaded into PDMS and PS chips and were incubated for 24 h. Bright-field and fluorescence (λ_{Ex} = 565 nm/λ_{Em} = 610/75 nm) images were taken. Fluorescence intensity profiles illustrate the distribution of the substances within the channels and into the wall materials over time. Sampling at t = 0 h was performed as fast as possible after filling the channels, but there was already diffusion into the wall material visible.

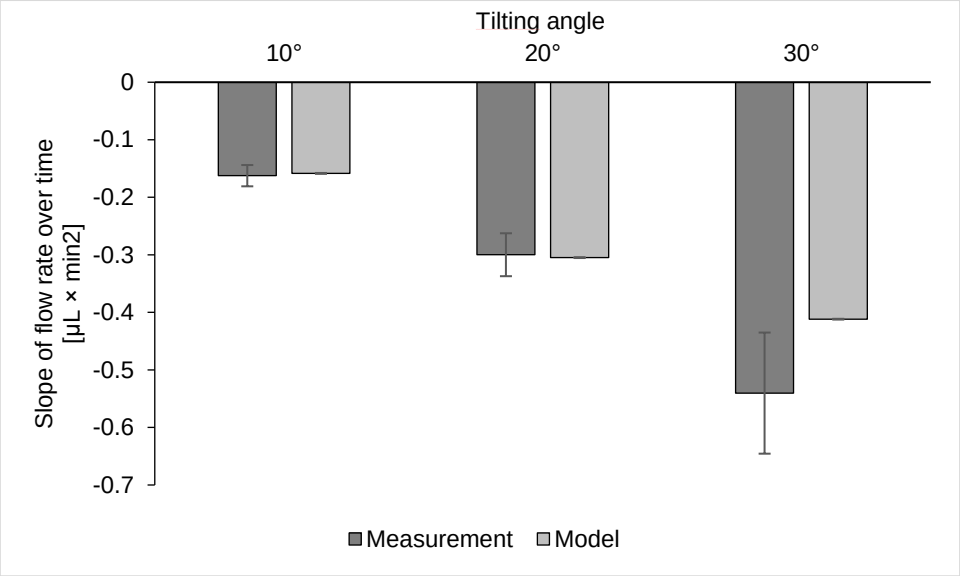

Supplementary Figure 2: Slopes of measured and modeled flow rates as a function of time at different tilting angles. The slopes of the measured flow rates match the modeled flow rates for tilting angles of 10° and 20°. The measured slope at 30° is steeper than the modeled one but also has a larger standard deviation than all other slopes.

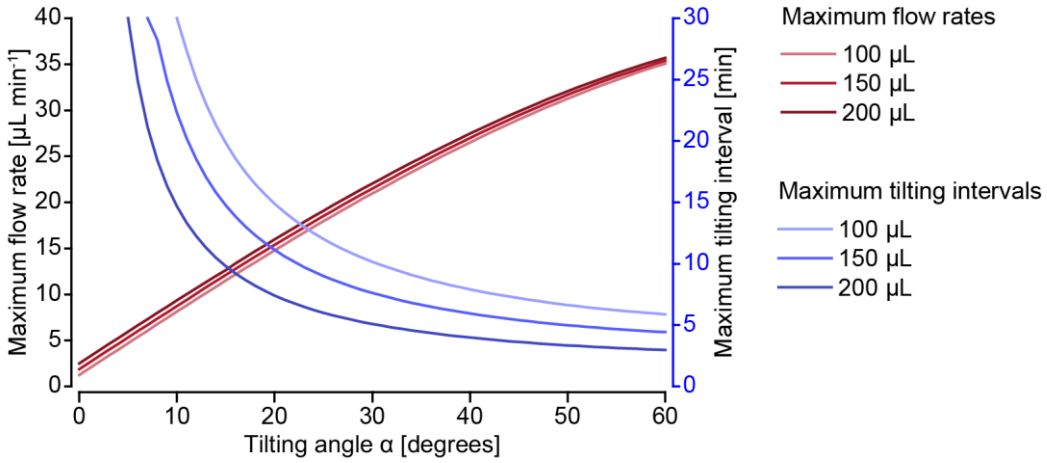

Supplementary Figure 3: The maximum flow rate and tilting interval until drainage of the top reservoir at 37 °C as a function of the tilting angle was calculated for initial liquid volumes of 100, 150 and 200 µL. Lower liquid volumes result in lower flow rates and shorter applicable tilting intervals.

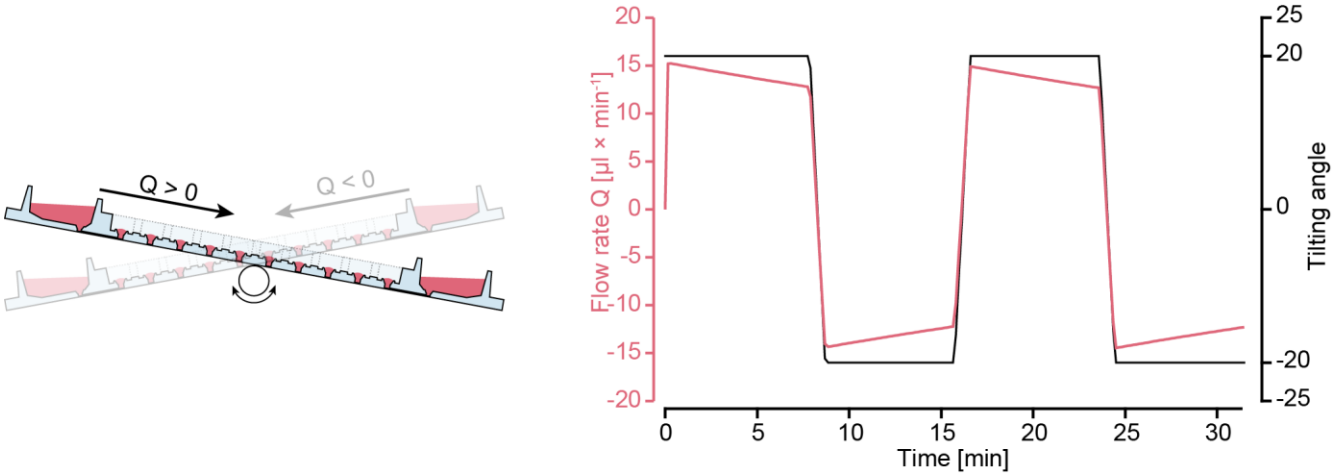

Supplementary Figure 4: Bidirectional flow rate through the channel upon repeated tilting over two tilting cycles with following parameters: tilting angle α = 20°, tilting interval = 7 min, transition time = 50 s.

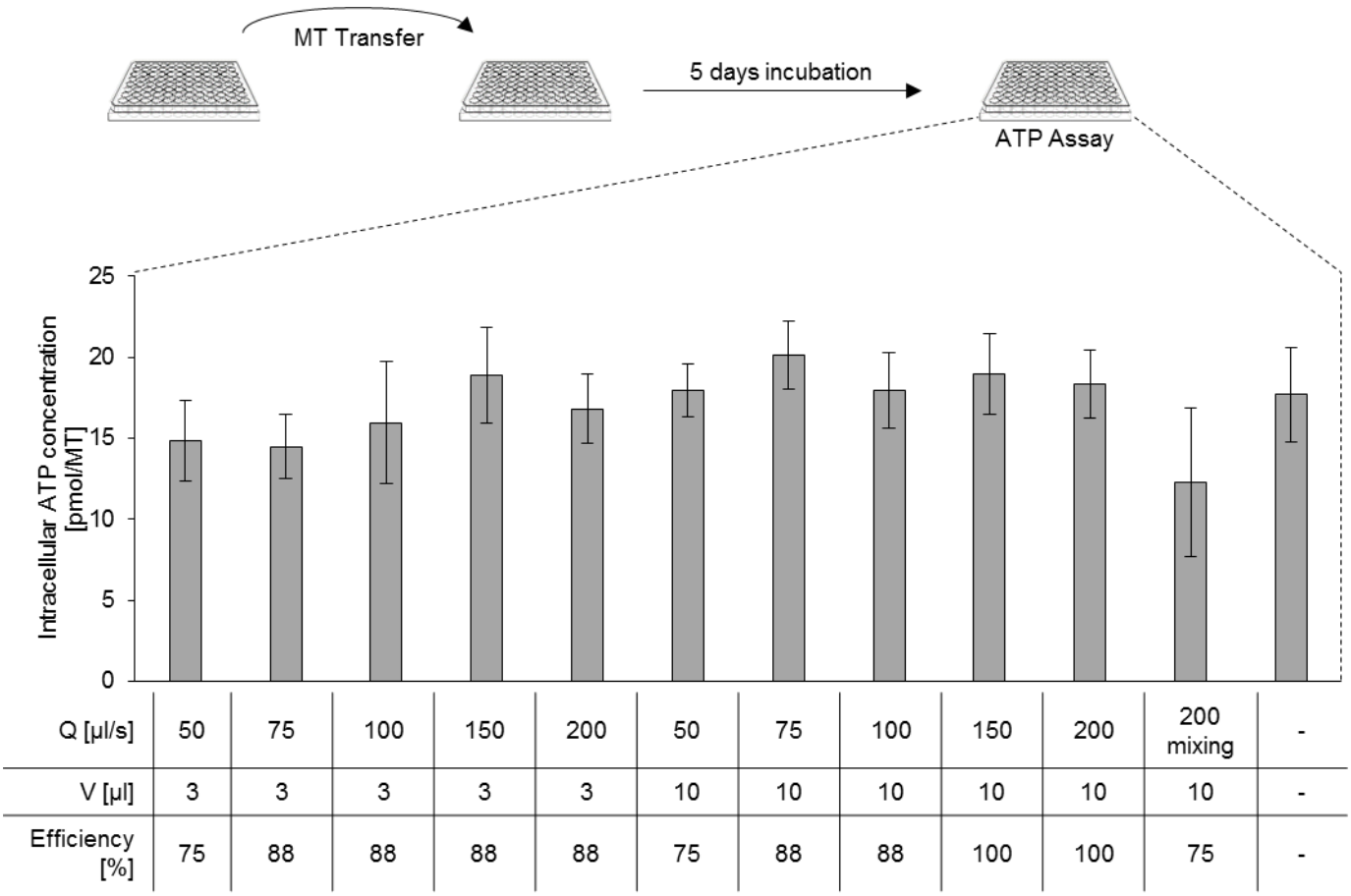

Q [µl/s]	50	75	100	150	200	50	75	100	150	200	200 mixing	-
V [µl]	3	3	3	3	3	10	10	10	10	10	10	-
Efficiency [%]	75	88	88	88	88	75	88	88	100	100	75	-

Supplementary Figure 5: Viability of human liver microtissues (hLiMTs) after transfer between two microtiter plates. hLiMTs were taken up with different uptake flow rates *Q* and uptake volumes *V* using an automatic liquid handling system (Hamilton STAR, Hamilton Bonaduz AG, Bonaduz, Switzerland). ATP-dependent viability shows no negative impact of high flow rates on hLiMTs during transfer as compared to the negative control that did not experience transfer. Transfer efficiency of up to 100 % could be achieved by taking up a volume *V* of 10 µL with a flow rate Q of 150 – 200 µl/s (n = 8 hLiMTs per data point; data represented as mean ± SD).

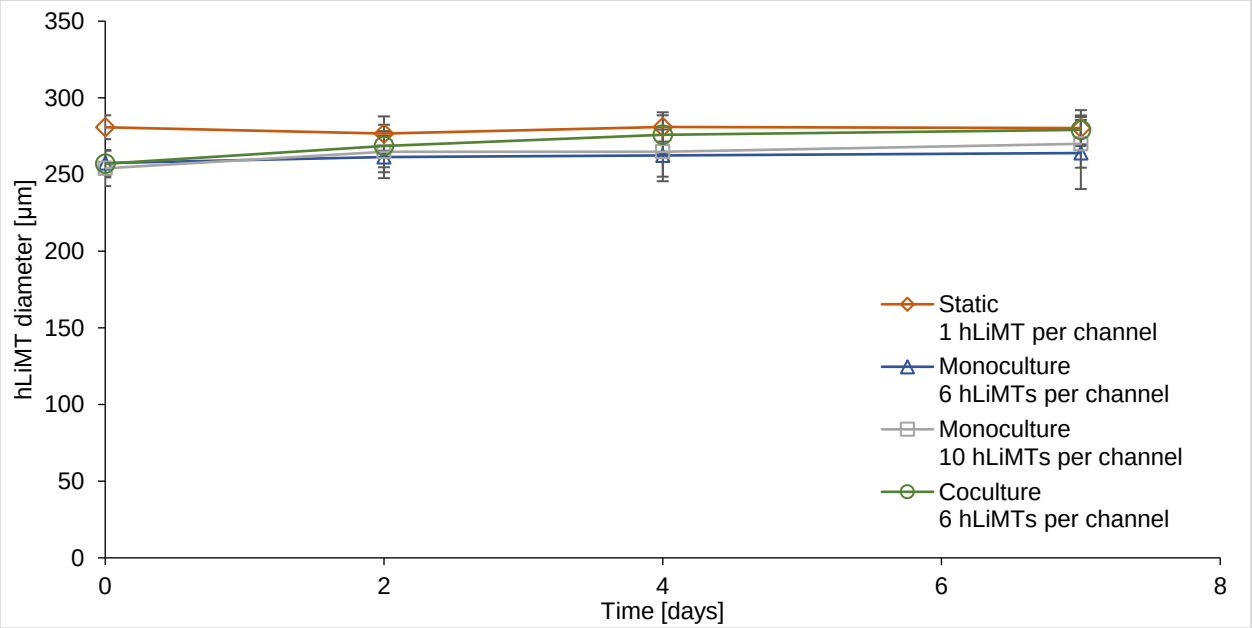

Supplementary Figure 6: Diameter of hLiMTs under static and perfused conditions over time. hLiMTs were cultured as one MT per well on a microtiter plate (orange) or as multiple MTs per channel on chip. Monoculture conditions included six (blue) or ten (grey) hLiMTs, and co-culture conditions (green) included six hLiMTs with four tumor MTs. The size of hLiMTs remained constant under all conditions over the experiment time (n = 8 – 40 hLiMTs per data point; data represented as mean ± SD).

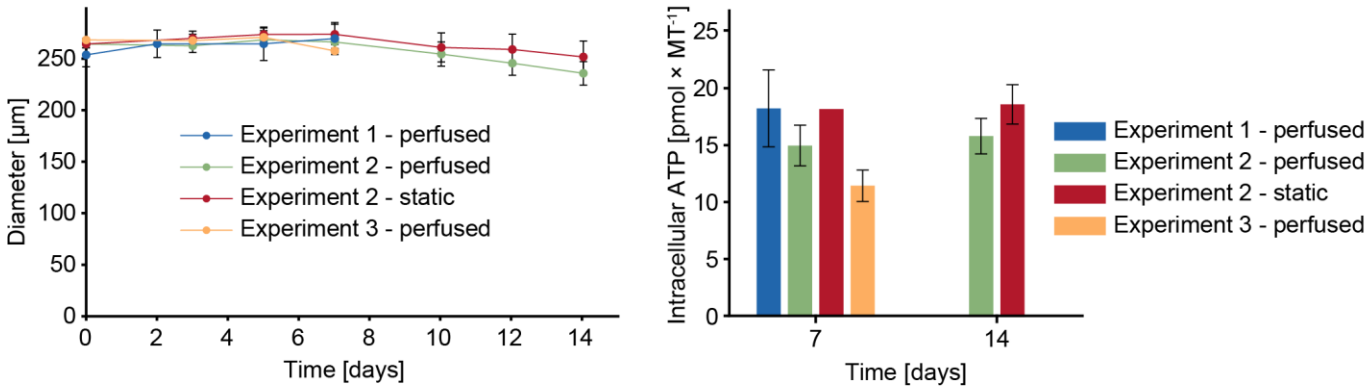

Supplementary Figure 7: Reproducibility of microtissue culturing within the microfluidic chip. 10 hLiMTs per channel were cultured in the microfluidic chip over up to 14 days in independent experiments in two different labs. (A) hLiMT diameter was tracked over time and (B) intracellular ATP concentrations were measured on days 7 and 14 (n = 40 – 80 hLiMTs per data point; data represented as mean ± SD).

Supplementary Movie 1: MT loading procedure using a 96-channel semi-automated pipetting system (VIAFLO 96/384, Integra Biosciences, Zizers, Switzerland). 80 MTs could be transferred from 96-well microtiter plates into the microfluidic chip in eight pipetting steps.

Supplementary Movie 2: Fully automated MT loading using a liquid handling robot (Hamilton STAR, Hamilton Bonaduz AG, Bonaduz, Switzerland), equipped with eight pipetting channels. Two types of MTs were transferred from individual 96-well microtiter plates for a co-culture configuration on the microfluidic chip.

Supplementary Movie 3: Rotating 3D animation of a tumor MT consisting of GFP-tagged MDA-MB-361 cells. The image stack was obtained on chip using an Olympus FV-MPERS system, equipped with a Newport SpectraPhysics DS+ 2-photon-laser and a XLPLN25XSVMP (25x, NA 1.0) water-immersed lens. (λ_{Ex} = 900 nm). The spatial resolution was 0.63 × 0.63 × 2 µm³. 119 images were acquired along the z-direction to cover the entire spheroid.